Spring 5-5-2015

Fracture Toughness of Irradiated Bone in a Murine Model

Lynda Marie Brady
Syracuse University

Fracture Toughness of Irradiated Bone in a Murine Model

A Capstone Project Submitted in Partial Fulfillment of the
Requirements of the Renée Crown University Honors Program at
Syracuse University

Lynda Marie Brady
Candidate for B.S. Degree
and Renée Crown University Honors
May 2015

Honors Capstone Project in Bioengineering

Capstone Project Advisor: _____
Kenneth A. Mann, Professor of Orthopedic Surgery, SUNY Upstate Medical University

Capstone Project Reader: _____
James H. Henderson, Associate Professor of Bioengineering, Syracuse University

Honors Director: _____
Stephen Kuusisto, Director

Date: 22 April 2015

Abstract

Cancer is a prevalent and diverse disease affecting fourteen million people in the United Sates alone. While some cancers can be treated effectively with one-time operations such as surgery, other cancers require more persistent treatments, commonly chemotherapy and radiation. These latter two treatments can have extreme side-effects and long-term ramifications. One long-term side effect of radiation therapy is a higher incidence of insufficiency fractures in bones of the skeleton. The mechanism responsible for this apparent weakness in bone is not well understood. In order to quantify changes in ductility following radiation therapy, femora from mice treated with 20 Gy radiation (with contralateral control) were subjected to three-point bend fracture toughness testing. A novel device for introducing a notch to the bones is presented in this study. Initiation fracture toughness was found to decrease 29% in irradiated bone compared to controls ($p=.03$). No significant difference was found in critical toughness or r-curve slope between control and irradiated bone. These results suggest that radiative therapy causes increased brittleness in cortical bone and could explain the increased incidence of fracture in patients treated with radiotherapy.

Executive Summary

Cancer is an increasingly common disease that, in addition to being a large focus of the scientific research community, has pervaded public consciousness as it has increased in prevalence. In 2014, 1.7 million new cases of cancer were diagnosed in the United States, while 12 million new cases were diagnosed worldwide.[1] [7] Of these patients, 52% will receive radiation therapy as part of their treatment to reduce tumor size, treat the entirety of the disease externally, or as a supplement to chemotherapy, surgery, or both.[7] In radiation therapy, high-energy beams of electromagnetic radiation, such as from X-rays or gamma rays, are introduced to a localized area of the body based on the location of the target cancer.[15] Radiation, while effective in treating some types of cancer, has long-reaching side effects, an issue common to many cancer treatments. One of these side effects is a higher incidence of insufficiency fractures, or fractures of bone resulting from weakened or damaged bone put under normal physiological stress.[17] These insufficiency fractures can dramatically affect quality of life, especially for patients who suffer pelvic fracture related to radiation therapy to treat gynecological, testicular, or colorectal cancers, rib fractures following treatment for breast cancer, or extremity fractures following treatment for sarcomas.[8]

In order to investigate the material properties of irradiated bone that may affect the resistance to fracture, fracture toughness tests were performed on irradiated and non-irradiated (control) bones to determine the difference in brittleness of the different bones. Irradiated-control pairs of adult Balb/C mouse femora were acquired from another study regarding the effects of radiation on bone at the Department of Orthopedic Surgery at SUNY Upstate Medical University. 20 Gy of radiation had been administered to the right hind leg of the mouse while the left leg was protected from the treatment. This allowed the left leg to serve as a control against

which the radiated bone could be measured. Mice were euthanized and limbs were harvested twelve weeks after radiation treatment. Femurs were frozen in saline soaked gauze to protect the integrity of the bone.

Previous studies on the effects of radiation on bone have included compression strength testing [21], biochemical testing[8] and morphological analyses[22], and suggested that irradiated bone is more brittle than normal bone. However, we did not find any previous testing of this hypothesis. Therefore, a fracture toughness test for the mouse femur was developed and performed in this study. Fracture toughness measures the resistance of a material to crack propagation or growth and thus resistance to fracture. The ability of a material to resist growth of a crack provides insight into the brittleness of the material. A more brittle material will have a lower fracture toughness value because the crack will grow faster and under conditions of less force than in a more ductile or malleable material. In order to perform this test, a small notch must be made in the bone to serves as the initiation point for crack propagation during mechanical loading.

While there are standardized procedures for testing fracture toughness of many man-made materials, there is no standard protocol for this type of test with a specimen on the scale of a mouse bone. Therefore, a procedure for making a small, sharp notch in the bone had to be developed. The designs were constrained by a need for feasibility of building the device, repeatability of results, the size of the samples, and the fragility of the samples. A small device was machined from plexiglass and aluminum to meet these requirements. Several blades were tested in order to find a notching protocol which would create a sufficiently sized notch in the bone.

After a sufficient notching device was created, a testing protocol was created. The bones were tested in a three-point bend set-up. In this three-point bend test, the bone rests on two small supports with an 8mm span, one on each end of the femur, and a force is applied directly between the two supports on the opposite side of the femur so that as the test progresses, the femur is bent into a U-shape, promoting growth of the crack through the cross section of the femur. The speed at which the sample is tested is critical because if the sample is tested too fast, the crack propagation will occur too fast to measure. Therefore, the test was run at a displacement rate of 0.075mm/min, meaning that a variable force was applied to maintain a constant displacement rate. This slow displacement rate balances the need to allow time for crack propagation with the constraint of running tests in a timely manner.

While the bones were loaded, pictures were taken with a high magnification camera so that the crack propagation through the bone could be seen. These pictures were taken every second and synced with the mechanical testing software so that the time readings of the data and the pictures would be comparable. The crack length was measured in each picture and used in conjunction with the force data to calculate the fracture toughness according to calculations reported by Ritchie et al.[18]

Based on previous literature regarding fracture toughness in murine models of other brittle bone diseases,[2] [3] [4] [5] [6] [14] [16] as well as the literature regarding mechanical and morphological changes in irradiated bone,[8] [22] the irradiated bones were hypothesized to have lower fracture toughness, indicating more brittleness in the material. This hypothesis has been supported by the data. In comparing left control limbs to right irradiated limbs on the same animal, irradiated bones consistently have a lower fracture toughness. Additionally, the resistance curve, the slope of which indicates ductility, is flatter for all irradiated specimens

compared to the control specimens. These results indicate that irradiated bone is more brittle than bone of normal physiological state.

These results offer insight into the mechanical differences between irradiated and normal bone, which can help direct hypotheses about the chemical, biological, and morphological changes that lead to the increase in insufficiency fractures in patients who undergo radiation therapy as a treatment for cancer. Hopefully, the results of this study can be used to identify and understand the cause of these changes and eventually reverse the damage to the patient or prevent it during treatment.

Table of Contents

Acknowledgements

I would like to thank the members of the Musculoskeletal Research Laboratory at the Institute for Human Performance at SUNY Upstate Medical University, especially Dr. Kenneth Mann and Jacklyn Goodheart, for providing superb mentorship as well as laboratory time, space, and supplies for this project. Without their help and support, I would not have been able to undertake such an endeavor. I would also like to thank my reader, Dr. James Henderson, for his helpful insight and keen eye in editing this work to add clarity, brevity, and logical flow. Finally, I would like to thank the Renee Crown Honors Program at Syracuse University for giving me the opportunity and motivation to perform and present this research and for fostering a community where I was able to grow academically and professionally within and far beyond the boundaries of my degree concentration.

Chapter 1

Introduction

Cancer is a prevalent disease in the United States as well as globally. 12 million new cases of cancer are diagnosed globally every year[7], with 1.7 million of these cases being diagnosed in the US[7]. Currently, 14 million people in the United States are currently living with a cancer diagnoses.[1] Common treatments for this widespread disease include surgery, chemotherapy, and radiation therapy. Radiation therapy is used in over 50% of cancers[7] to shrink local tumors for easier surgical removal or to remove the cancer entirely. However, use of radiation therapy for soft tissue cancers can have a detrimental effect on underlying bone structures.[8] Radiation therapy has been linked to higher incidence of insufficiency fractures, the cause of which is unknown.[22] Prior work suggests that bone subjected to radiation displays significant chemical and morphological differences from normal bone, and more brittleness than normal bone.[8] [22]

Previous studies on both whole body and localized radiation have concluded that radiation can both inhibit osteoclast differentiation and induce osteoblast differentiation, leading to an increase in total bone mass at short times after irradiation, which will rebalance after a period of time.[8] Additionally, radiation causes an embrittlement of bone, possibly caused by increased collagen interlinking.[8] [22] These proposed physiological changes in bone correspond to changes in strength of the samples tested by tensile or compressive stress tests. However,

fracture mechanics testing can provide an advantage over the strictly tensile, compressive, or torsional tests in previous studies by accounting for the micro-crack flaws in bone.[20]

Fracture toughness is a measure of resistance of a material to brittle fracture. Fracture toughness measurements give insight into strength, elasticity, and ductility of materials in a way that simpler tensile and compressive strength tests cannot. Fracture toughness testing does not measure the gross material strength but rather the ability of the material to dissipate high localized stress over a small area around a defect. Methods of fracture toughness testing therefore involve adding a sharp notch or "pre-crack" to a testing material in order to control the initiation of the fracture pattern of the sample. Fractures begin at sites of existing flaws in the material. A sharp pre-crack or notch can supersede these natural surface deformations of a material, allowing researchers to follow the crack propagation and match the propagation to applied loads. The relationship between crack propagation and load can thus be obtained for the duration of the test. Because the fracture toughness of a material is more dependent on the mechanical properties of the material microstructure, such a test is a more informative measure of brittleness than tensile or compressive stress testing.[18]

Fracture toughness tests are commonly performed on materials, including bone, to measure changes in ductility. However, the use of fracture toughness testing in small animal models is a relatively recent endeavor. The need for a sharp notch which is very small in size relative to the tested specimen has been a source of difficulty in performing these tests.[19] However, several additions to the literature in the past ten years have used murine models to measure fracture toughness in wild type mice as well as with reference to brittle bone diseases such as osteogenesis imperfecta and rheumatoid arthritis.[2] [3] [4] [5] [6] [14] [16] [18]

In order to further understand the relationship between radiation and brittleness leading to insufficiency fractures, this study performed fracture toughness tests on mouse femora treated with therapeutic levels of radiation. Following the literature on biological effects of radiation on bone, correlation of insufficiency fractures in radiation-exposed bone, and the differences in fracture toughness between wild type and brittle bone murine models, we hypothesize that the irradiated femora will exhibit lower fracture toughness values than non-irradiated femora.

Chapter 2

Methods and Materials

Notching Device

A novel device was produced for the purpose of creating an initial notch in the diaphysis of a mouse femur. A block was cut from a 25 mm Plexiglas sheet using a band saw, and the edges were squared with a milling machine. The center of the Plexiglas block was located, marked, and scored before the mill was used to create a 1/2” hole at the center which penetrated about halfway through the material. An NC7 hole was drilled opposite the ½” hole until the two holes met. A ¼” tap was used to thread the NC7 hole, and a set screw was added to the NC7 hole so that the depth of the ½” hole could be adjusted as needed. Four blocks were cut from a

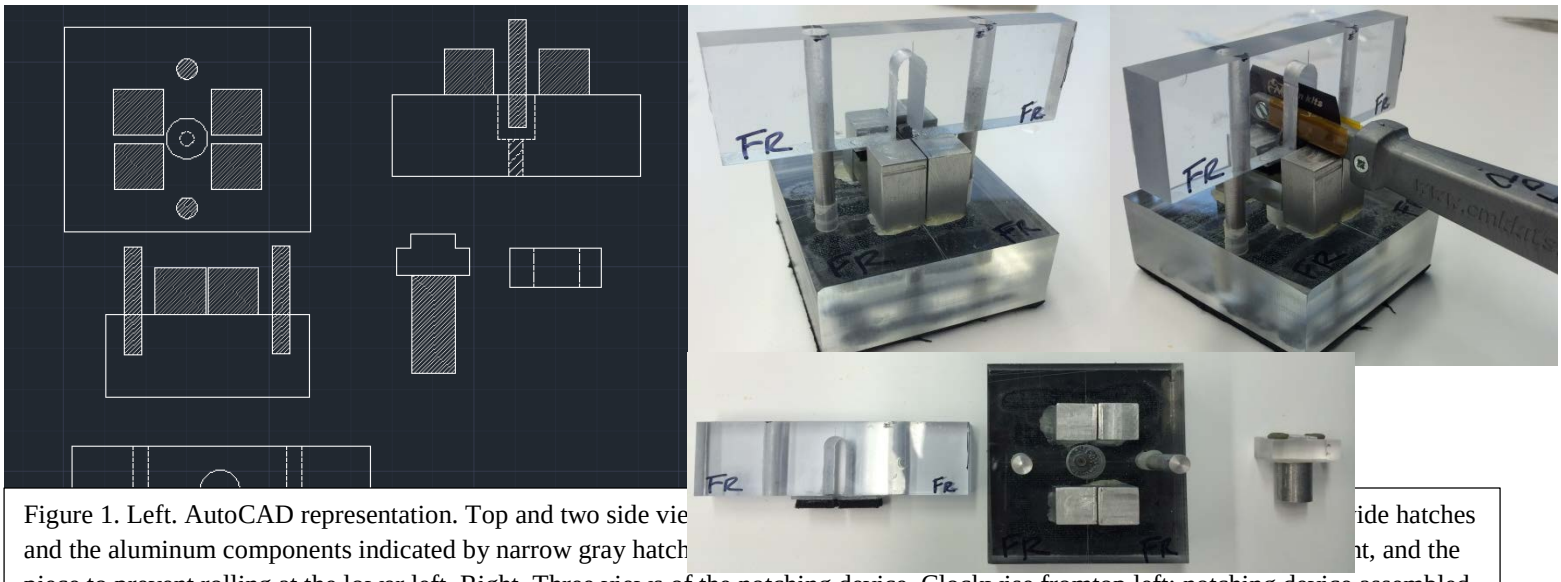

Figure 1. Left. AutoCAD representation. Top and two side vie ide hatches and the aluminum components indicated by narrow gray hatch nt, and the piece to prevent rolling at the lower left. Right. Three views of the notching device. Clockwise fromtop left: notching device assembled for notching, no blade, notching device assembled for notching with blade, notching device in parts. Clay used for holding bone in position can be seen on the pedestal at the right of the bottom picture.

rectangular aluminum bar and subsequently smoothed with sandpaper. The blocks were arranged two each on opposite sides of the center hole and aligned so that on each side, one aluminum block was on one side of the center score and the other was on the other side. The aluminum blocks were secured with epoxy and allowed to set. These blocks were spaced .20mm apart using a razor blade so that during testing, the handle of the blade would act as a stop for the blade, ensuring reproducibility of results. A block of plexiglass was machined so that a raised portion would support the bone while the condyles would rest over the edge, allowing for notching without stressing the bone. A 10" tall, ½" diameter cylindrical aluminum piece was attached to the machined plexiglass piece. Modelling clay was placed on the lowered sides of the plexiglass piece to hold the bone securely during notching. A third plexiglass block was created as a securing device to prevent rolling of the bone during notching. This block was machined using a bandsaw, and ¼" holes were drilled into the block so that the block could slip smoothly over two ¼" aluminum rods added to the sides of the ½" hole in the base. A channel was cut into the block so that the blade could run through the plexiglass. Foam strips were adhered to the bottom of the block so that the device would not compromise the bone.

Notching Blade

In order to perform an accurate fracture toughness test, a blade was required which would make a sharp enough notch relative to the size of the sample without sacrificing ease of cutting so as not to put too much stress on the sample prior to testing. Four blades were initially tested: a 0.27 mm kerf serrated blade, a 0.20 mm kerf razor blade, a 0.15 mm kerf razor blade, a 0.13mm serrated blade, and a scalpel blade. Variations on these blades were also tested, including blades filed down on both sides by holding the blade at an angle against a polisher, leading to a serrated blade with a sharp tip more characteristic of a razor blade.

Animals

Fifteen pairs of frozen Balb/C mouse femora were obtained from a prior experiment by Wernle el al. at SUNY Upstate Medical University. In this IUCAC-approved protocol, right limbs were treated with 20 Gy radiation prior to euthanization at 12 weeks post-irradiation treatment while left limbs were protected from treatment. The femora were received frozen in saline-soaked gauze to preserve bone integrity.

Fracture Toughness Testing

Bones were thawed as needed and notched on the anterior side. Femora were soaked in a saline solution before being loaded into the three-point bend system in a QT/1L Q-Test MTS machine. The three point bent set up was comprised of two supports with an 8mm span fixed to the MTS plate and a mechanically controlled element of similar size aligned

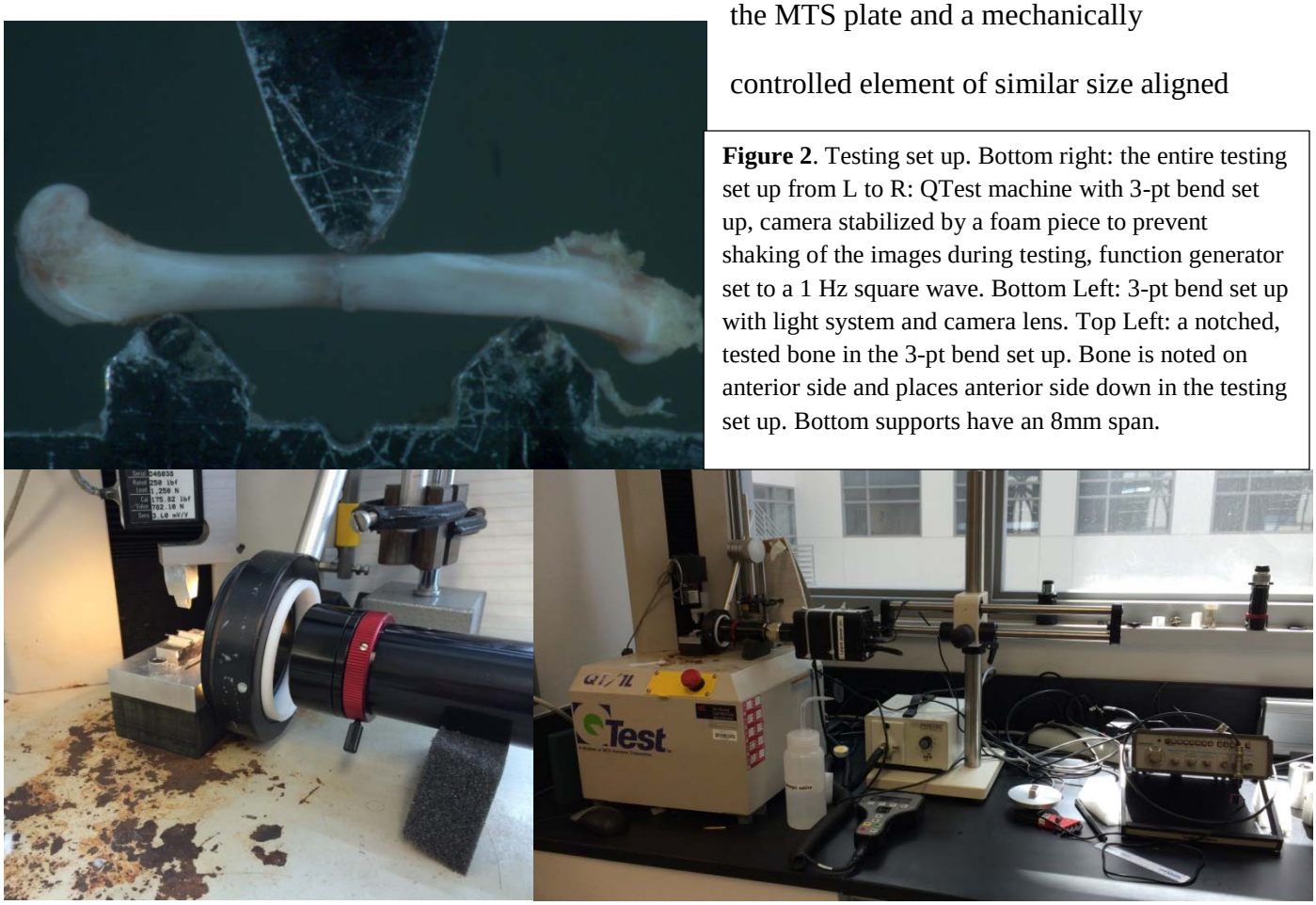

Figure 2. Testing set up. Bottom right: the entire testing set up from L to R: QTest machine with 3-pt bend set up, camera stabilized by a foam piece to prevent shaking of the images during testing, function generator set to a 1 Hz square wave. Bottom Left: 3-pt bend set up with light system and camera lens. Top Left: a notched, tested bone in the 3-pt bend set up. Bone is noted on anterior side and places anterior side down in the testing set up. Bottom supports have an 8mm span.

to apply the force to the bone directly between the two supports. (Figure2) Bones were loaded anterior side down. After the bones were pre-loaded to 1 N, a function generator signaled the simultaneous start of loading a rate of .075 mm/min and capture of photos at a rate of 1 Hz with a camera, synching the mechanical and pictorial data. The camera was fitted with a magnifying lens to overcome the challenge of capturing crack propagation on the small scale of a murine model. The displacement, load, and time were recorded through TestWorks. The peak load, break load, and corresponding energies were calculated in TestWorks and recorded. After mechanical testing was complete, a picture of the bone cross section at the crack site was taken, and the bone diameter was measured using calipers. These images and measurements were used to calculate further bone geometries needed for fracture toughness calculations.

Data Processing

The photographs were imported into Image J, where crack length and geometry measurements were taken, and the crack propagation was observed. Measurements of the notch propagation and bone geometry were used in combination with mechanical load data to calculate fracture toughness according to methods described by Ritchie et al.[3] [17] where the fracture toughness, K, was calculated using the equation

$$K=F_b \frac{PSR_o}{\pi(R_o{}^4-R_i{}^4)}\sqrt{\pi R_m \theta}$$

where θ is the half crack angle, R_m is the mean radius of the diaphysis, R_o is the outer radius of the diaphysis, R_i is the inner radius of the diaphysis, P is the load on the bone at the time and

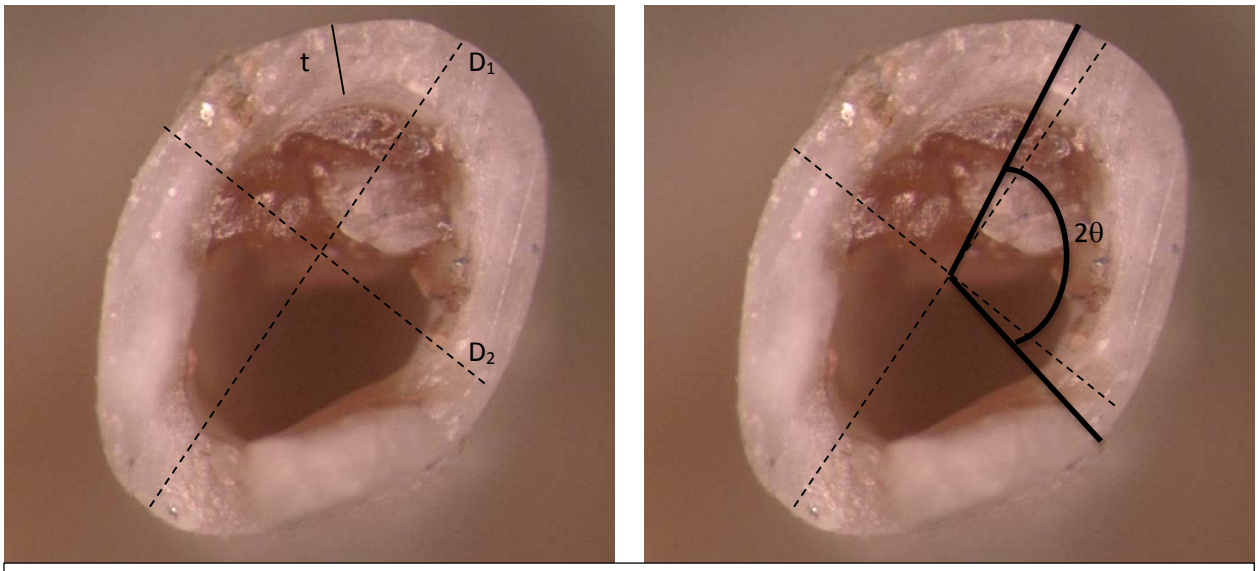

Figure 3. Cross-section of bone. Left. Measurements taken from the cross sectional images. D1 is the larger elliptical diameter, D2 is the smaller elliptical diameter. These values were averaged to obtain Ro. t is a sample thickness measurement. 4-6 thickness measurements were averaged to obtain a thickness value. Right. The initial crack angle 2θ. The half crack angle θ was calculated using methods described.

displacement being calculated, and S is the span of the testing set up. F_b is a constant defined by the geometry of the specimen, here assumed to be a thick-walled pipe and given by

$$F_b=(1+\frac{t}{R_m})[A_b + B_b(\frac{\theta}{\pi}) + C_b(\frac{\theta}{\pi})^2 + D_b(\frac{\theta}{\pi})^3 + E_b(\frac{\theta}{\pi})^4]$$

where the constants A_b, B_b, C_b, D_b, and E_b are determined by the geometry and dependent on the thickness and mean radius. The half-crack angle θ for this study was calculated using the following equation rather than the method presented in the Ritchie text:

$$\theta = \sqrt{\frac{R_m{}^2-(R_o-a_s)^2}{R_o-a}}$$

where θ is the half crack angle, R_m is the mean radius, R_o is the outer radius, a is the crack length as viewed from the camera and measured from the base of the specimen, and a_s is the scaled crack length adjusted for the non-circular geometry of the bone. The outer radius was calculated by averaging using appropriate equations on two diameter measurements, the diameter of the bone along the longer elliptical axis of the diaphysis (D_1) and the diameter of the bone measured

along the shorter elliptical axis of the diaphysis (D_2), which were obtained externally using calipers. The thickness of the cortical bone was not uniform. Thus, the thickness was determined using an average of several thickness measurements taken from around the circumference of the cross section where the notch was placed and subsequent fracture occurred. The inner radius was obtained by subtracting the thickness from the outer radius. All quantifying geometric calculations performed Image J were based off of one of two physical measurements:. The fracture toughness was calculated for every image where the crack was propagating. The initiation toughness (K_{int}) was calculated using the half-crack angle and load at the start of crack propagation, and the critical or instability fracture toughness (K_{crit}) was calculated using the peak load and the crack length just before failure, or growth instability. Calculations were performed in Microsoft Excel. The fracture toughness for each specimen was plotted against the change in crack length from frame to frame to obtain the resistance curve (R-curve). The slope for the R-curve was calculated using a linear regression fit in Microsoft Excel.

Statistics

The mean and standard deviation of the initiation fracture toughness, the critical fracture toughness, and the slope of the rising r-curve were calculated in Excel. All properties recorded from the mechanical testing machine, including peak load, break load, stiffness, energy to peak and break, and elongation to peak and break were similarly analyzed. Data from trials in which the bones rotated or no crack propagation occurred were excluded from calculations. A two sample, two-tail t-test was performed in Microsoft Excel for the K_{int}, the K_{crit}, and the slope as well.

Chapter 3

Results

Notching Blade

Of the initial five blades, none was found to create a satisfactory notch. The serrated blades easily cut through the sample toothpicks and the sample of bone. However, the serrated blades left square-bottomed cuts, which were not sharp enough to initiate crack propagation. The razor blades were difficult to use and did not cut through the toothpicks or the bone sample very well. However, though the razor blades made very shallow cuts after more strokes than the serrated blades, the cuts were much sharper. (Figure 2) Therefore, since the 0.13mm serrated blade had both the advantage of ease-of-use and the thinnest kerf, it was filed to a point using a

Figure 4. Top Right. Five cuts made by initial blades, from le mm serrated. Bottom Right. Cut made by "hybrid" polisher-filed blade. Bottom Middle. Final notch design made from using the filed serrated blade and the thinner razor blade. Left. Two blades used for notching. The bottom blade is serrated to aid ease of notching and was filed on a polisher to reduce width. The top blade is thinner and was used to add a sharp tip to the notch.

polishing blade to create a hybrid serrated-razor blade. This custom blade created a sharp, narrow notch with relative ease and minimized the number of strokes required to cut through the cortical bone. However, the blade could not be filed sharp enough for the necessary use. Therefore, a second blade was introduced. This thinner, non-serrated blade was used after the custom blade to create a sharper tip in the notch. (Figure 4)

Fracture Toughness Tests

Fracture toughness values obtained ranged from 1 to 6 MPa·mm$^{1/2}$ in irradiated bone and from 1 to 8 MPa·mm$^{1/2}$ in control bone, encompassing a wider range than reported in the literature. These data also showed larger variance than that found in the literature for comparable tests. The overall mean value for fracture toughness was comparable to values reported previously for wild type, and the mice mean values of the initiation and critical fracture toughness for control bones were comparable to values reported previously for C7BL/J6 mice. The mean value for irradiated bone was comparable to the mean value reported by Carriero et al for oim/oim mice and Davis et al for Brtl/+ mice. No significant differences were found between control and irradiated bones in the mechanical parameters of peak load, break load, stiffness, energy to peak, energy to failure, or elongation to peak and failure. Differences between critical fracture toughness of the irradiated and control femurs and the slope of the rising r-curves between the irradiated and control femurs were not significant. The initiation toughness was found to be 1.07 MPa/m$^{1/2}$ lower in the irradiated bones than in the control bones ($p < .05$).

	Kint (MPa·mm$^{1/2}$)	**Kcrit (MPa·mm$^{1/2}$)**	**Slope (MPa·mm$^{1/2}$/t))**
RTx	2.51±1.03	4.53±1.15	9.16±4.58
Control	3.67±1.31	5.52±2.28	12.78±3.45

Table 1. Initiation toughness, critical toughness, and r-curve slope for irradiated and control bones.

Table 2. Other recorded mechanical parameters for irradiated and control bones.

	Peak load (N)	Stiffness (N/m)	Break load (N)	Energy to Break (N·mm)	Energy to Peak (N·mm)	Elongation at Peak (mm)	Elongation at Break (mm)
RTx	4.21±1.18	80.4±15.6	3.82±1.27	0.21±0.08	0.16±0.09	0.07±0.01	0.08±0.02
control	4.79±1.27	94.46±25.1	3.73±2.11	0.20±0.09	0.14±0.08	0.07±0.02	0.07±0.02

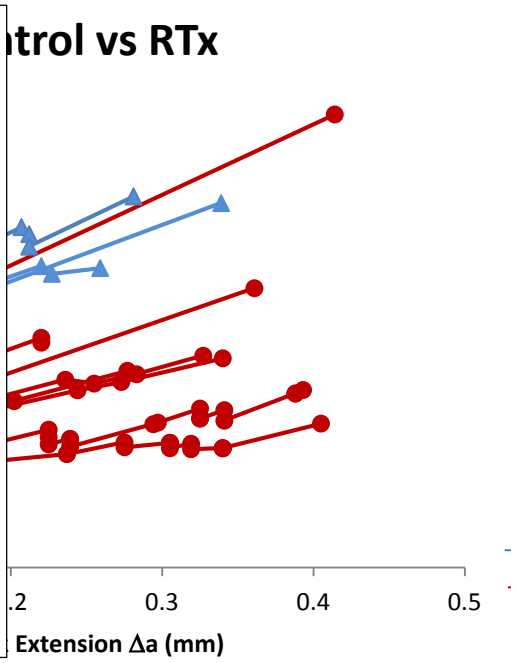

Figure 5. Fracture toughness as a function of crack extension. The Control vs RTx graph shows the general grouping of irradiated bones at lower fracture toughness values than the non-irradiated bones. The combined graph also illustrates the generally steeper R-curves seen in the control bones and the flatter curves seen in the irradiated bones. The separate RTx and Control graphs show the higher variability of the non-irradiated bones compared to the irradiated bones. All three graphs display the larger variance observed in critical toughness versus initiation toughness.

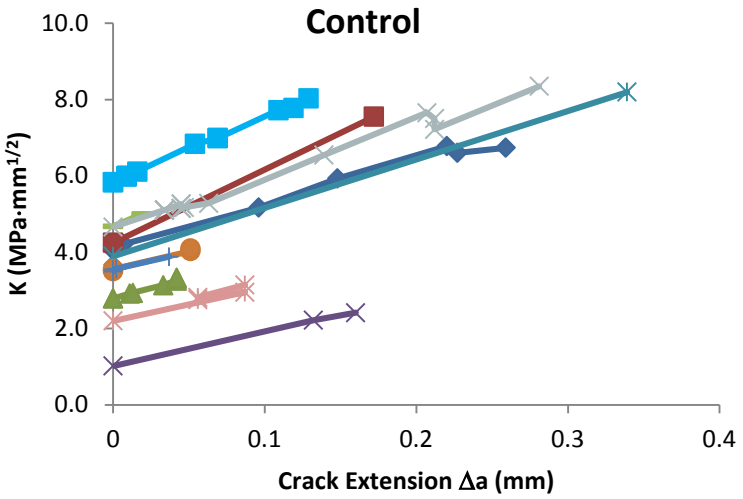

Figure 6. Crack propagation through bone during testing, progressing from initial synthetic notch created using novel system described in this study to failure. Crack propagation is clearly visible and measureable.

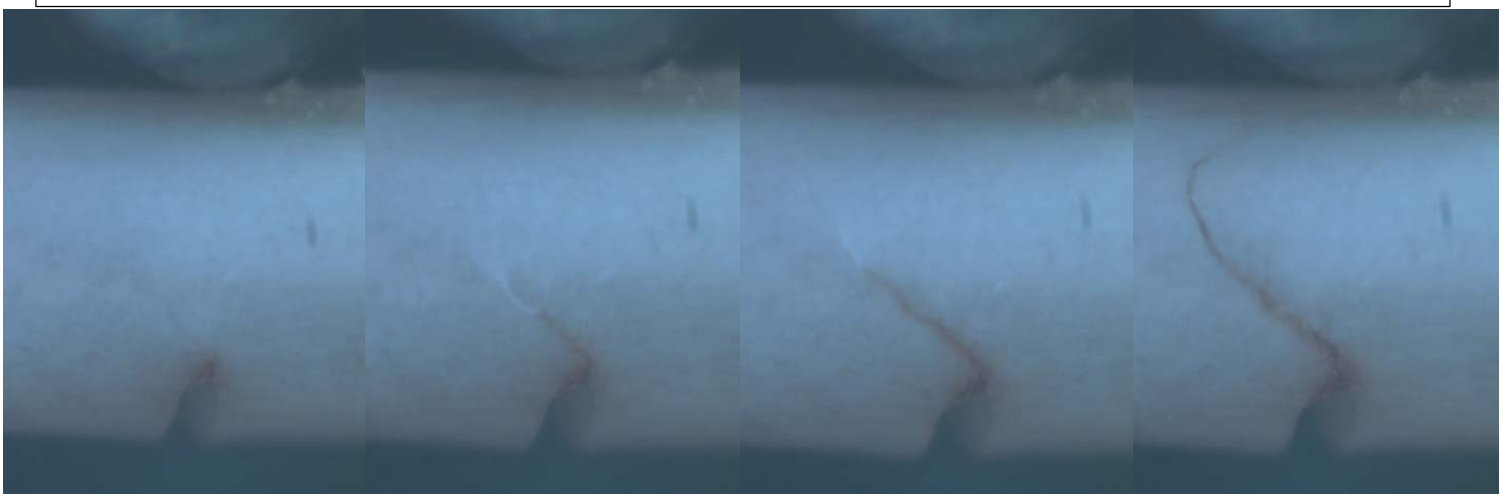

Chapter 4

Discussion

The use of radiation therapy as a treatment for cancer has been shown to have significant long-term effects, including increased incidence of insufficiency fractures. However, the mechanical and morphological changes of bone exposed to therapeutic levels of radiation and their causes are not well understood. Previous work has indicated that bone may become more brittle as a result of exposure to therapeutic radiation,[22] and a hypothesized causal factor of this change is increased collagen crosslinking.[8]

Our results support the hypothesis of increased brittleness of bone. The initiation toughness was 29% lower in the irradiated bones compared to the control bones, indicating that less energy was needed to initiate crack propagation in the irradiated bones than in the control bones. This corresponds to lower energy needed to overcome the resistance of the material and thus less ductility. The mean fracture toughness value obtained in this study is comparable to the mean value obtained by Carriero et al[4] for oim/oim mice, which are a model of osteogenesis imperfecta, a brittle bone disease.

The critical fracture toughness showed much more variation and therefore no significant difference was found. This apparent discrepancy in fracture toughness trends could be explained by low resolution in the testing method. While the rate of loading was decreased significantly for this application, the crack propagation still proceeded rapidly. The image sampling rate of 1Hz

was too slow in some applications to get an accurate depiction of the crack propagation. In these instances, the change in force was difficult or impossible to accurately match to a crack length. The speed of testing also varied depending on the hydration of the bone, which itself depended on the speed of test set-up. In future work, a continuously hydrating device or a higher image sampling rate might reduce variability between specimens.

Additionally, the resolution of the images and focus of the camera was not consistent. In trials where the bone shifted during pre-load or testing or the camera moved during testing, the focus of the camera moved out of focus, making determination of propagation initiation and measurement of crack length difficult. The small scale of the sample and the necessity for high magnification made camera stability, especially in conjunction with a motor powered mechanical testing system, difficult. In future studies, efforts should be made to stabilize the camera during testing to avoid focal clarity issues. The camera focus in this study was adjustable between preload and testing, but could not be adjusted once testing began. In future studies, efforts should be made to refocus the camera after pre-loading, and different image capture software should be investigated in order to find a program which allows viewing of real-time images during testing and refocusing of the camera during testing.

The resistance curve (R-curve), created by plotting the fracture toughness against the change in crack length, offers insight into the brittle nature of a material subjected to a fracture toughness test. In an ideal brittle material, the r-curve will be flat. A rising R-curve indicates presence of ductility in the material. While the sample tested in this experiment did not show statistically significant differences in R-curve slope between the two groups, the radiation-treated samples did have generally lower R-curve slopes. In the future, the sample size should be increased to reduce the effects of variation and determine if there is a significant correlation

between radiation treatment and a milder R-curve slope. Increased sample size could also help to solidify the conclusion that the initiation toughness is significantly lower in the irradiated bones, and could lend insight into the effect of radiation on critical fracture toughness.

Inconsistencies across parameters could be explained in part by error introduced by assumptions in the equations and by the method of notching. Equations used in this study assume a circular cross sectional geometry for the bone. However, the cross-sectional geometry of bone is generally elliptical and highly variable depending on position in the diaphysis. Cross sections closer to the femoral head will have a more elliptical and less regular shape than cross sections nearer to the distal articulating surface of the femur. Therefore, the assumption that the cross sectional geometry is circular introduces error into the equation, and this error varies over the length of the bone. A worst-case error propagation done by Ritiche et al. estimated 17% error due to geometry differences between long bones and the circular cross-section approximation. Additionally, the equations are based on a thick walled pipe approximation in which the thickness is uniform throughout the sample. However, the thickness of the cortical wall of the femur varies depending on position in two axes, both by location on the diaphysis proximally to distally and radially. Therefore, the average thickness of the cortical wall used in the equation may not be an accurate approximation of the wall thickness for every point at which the fracture toughness was calculated.

Another potential source of error was the variability in notch length. Although the notching device was designed to consistently produce uniform cracks, in practice the variation between bone diameters caused significant variations in notch depth as evidenced by the value of the standard deviation of these measurements being 58% of the value of the mean (0.313 mm ± 0.247 mm), as well as the range of these measurements (0.667 mm) A positive correlation

between was found between length of the notch and the initiation toughness. This correlation was unexpected and should be investigated further in future studies.

Although this study failed to account for the sources of error described above, the results support the hypothesis that therapeutic radiation leads to a decrease in fracture toughness. While this thesis is only supported by these data in initiation toughness, the rest of the data suggest support in the other parameters as well. Taken in combination with previously published results, these data suggest that therapeutic radiation treatment for cancer is likely to cause decreased ductility in treated bone as well as bone underlying treated tissues.

Works Cited

[1] "Cancer Prevalence: How Many People Have Cancer?" *Cancer Prevalence: How Many People Have Cancer?* American Cancer Society, n.d. Web. 20 Oct. 2014.

[2] Carriero, A., E. A. Zimmermann, A. Paluszny, S. Y. Tang, H. Bale, B. Busse, T. Alliston, G. Kazakia, R. O. Ritchie, and S. J. Shefelbine. "How Tough Is? Investigating Osteogenesis Imperfecta in Mouse Bone." *Journal of Bone and Mineral Research* (2014): 1392-1401. Web.

[3] Carriero, Alessandra. "Is Microindentation Indicative of Fracture Toughness in Mouse Bone." *Speakers*. Orthopaedic Research Society, n.d. Web. 12 Mar. 2014.

[4] Alessandra, Carriero, Jan L. Bruse, Karla J. Oldknow, Jose Luis Milan, Colin Farquharson, and Sandra J. Shefelbine. "Reference Point Indentation Is Not Indicative of Whole Mouse Bone Measures of Stress Intensity Fracture Toughness." *Bone* 69 (2014): 174-79. *Eslevier*. Web. 13 Apr. 2015.

[5] Davis, Mathieu S., Bethany L. Kovacic, Joan C. Marini, Albert J. Shih, and Kenneth M. Kozloff. "Increased Susceptibility to Microdamage in Brtl/ Mouse Model for Osteogenesis Imperfecta." *Bone* 50.3 (2012): 784-91. *Elsevier*. Web. 13 Apr. 2015.

[6] Delaney, Geoff, Susannah Jacob, Carolyn Featherstone, and Michael Barton. "The Role of Radiotherapy in Cancer Treatment." *Cancer* 104.6 (2005): 1129-137. *Wiley Online Library*. Web.

[7] Fondy, Thomas P. *The Biology of Cancer: Introduction to BIO 501* [PDF document]. Retrieved From Lecture Notes Online Website: http://tpfondy.syr.edu/bio501/501Syl15.htm

[8] Gong, Bo, Megan E. Oest, Kenneth A. Mann, Timothy A. Damron, and Michael D. Morris. "Raman Spectroscopy Demonstrates Prolonged Alteration of Bone Chemical Composition following Extremity Localized Irradiation." *Bone* 57.1 (2013): 252-58. Print.

[9] Horton, Jason A., Kathryn E. Hudak, Eun Joo Chung, Ayla O. White, Bradley T. Scroggins, Jeffrey F. Burkeen, and Deborah E. Citrin. "Mesenchymal Stem Cells Inhibit Cutaneous Radiation-induced Fibrosis by Suppressing Chronic Inflammation." *Stem Cells* 31.10 (2013): 2231-241. Print.

[10] Katsamenis, Orestis L., Thomas Jenkins, Federico Quinci, Sofia Michopoulou, Ian Sinclair, and Philipp J. Thurner. "A Novel Videography Method for Generating Crack-Extension Resistance Curves in Small Bone Samples." *National Center for Biotechnology Information*. U.S. National Library of Medicine, 06 Feb. 2013. Web. 12 Mar. 2014.

[11] Koester, Kurt J. "The Fracture Properties and Toughening Mechanisms of Bone and Dentin." *Google Books*. ProQuest LLC, n.d. Web. 12 Mar. 2014.

[12] Kruzic, J. J., Kuskowski, S. J. and Ritchie, R. O. (2005), Simple and accurate fracture toughness testing methods for pyrolytic carbon/graphite composites used in heart-valve prostheses. J. Biomed. Mater. Res., 74A: 461–464. doi: 10.1002/jbm.a.30380

[13] Lendhey, Martin. "Bone Tissue Quality Determination of Mice Through a Novel Reference Point Indentation Technique." Diss. The City College of New York, 2011.

Bone Tissue Quality Determination of Mice Through a Novel Reference Point Indentation Technique. 2011. Web. 12 Mar. 2014.

[14] Makowski, Alexander J., Sasidhar Uppuganti, Sandra A. Wadeer, Jack M. Whitehead, BArbara J. Rowland, Mathilde Granke, Anita Mahadevan-Jansen, Xiangli Yang, and Jeffry S. Nyman. "The Loss of Activating Transcription Factor 4 (ATF4) Reduces Bone Toughness and Fracture Toughness." *Bone* 62 (2014): 1-9. *Elsevier*. Web. 13 Apr. 2015.

[15] Mayo Clinic Staff. "Radiation Therapy." *Mayo Clinic*. Mayo Foundation for Medical Education and Research, n.d. Web. 13 Apr. 2015.

[16] Mcnerny, Erin M. B., Bo Gong, Michael D. Morris, and David H. Kohn. "Bone Fracture Toughness and Strength Correlate with Collagen Cross-Link Maturity in a Dose-Controlled Lathyrism Mouse Model." *Journal of Bone and Mineral Research* (2014): 455-64. Web.

[17] Pentecost RL, Murray RA, Brindley HH. Fatigue, Insufficiency, and Pathologic Fractures. *JAMA.* 1964;187(13):1001-1004

[18] Ritchie, R.O., K.J. Koester, S. Ionova, W. Yao, N.e. Lane, and J.W. Ager. "Measurement of the Toughness of Bone: A Tutorial with Special Reference to Small Animal Studies." *Bone* 43.5 (2008): 798-812. Print.

[19] "Surveillance, Epidemiology, and End Results Program Turning Cancer Data Into Discovery." *Cancer of All Sites*. National Institute of Health, n.d. Web. 12 Mar. 2014.

[20] Vashishth, Deepak. "Small Animal Bone Biomechanics." *Bone* 43.5 (2008): 794-97. Print.

[21] Voide, Romain. "Diss. ETH No. 17524 Functional Phenotyping of Bone: A Hierarchical Assessment of Bone Failure Characteristics." Thesis. ETH Zurich, 2007. ETH Zurich. Web. 12 Mar. 2014.

[22] Wernle, James D., Timothy A. Damron, Matthew J. Allen, and Kenneth A. Mann. "Local Irradiation Alters Bone Morphology and Increases Bone Fragility in a Mouse Model." *Journal of Biomechanics* 43.14 (2010): 2738-746. Print.

[23] Xiao, Keqin, Lin Ye, and Yuk S. Kwok. "Effects of Pre-cracking Methods on Fracture Behaviour of an Araldite-F Epoxy and Its Rubber-modified Systems." *Journal of Materials Science* 33.11 (1998): 2831-836. *Springer Link*. Web. 12 Mar. 2014.

[24] Yahyazadehfar, M., A. Nazari, J. J. Kruzic, G.D. Quinn, and D. Arola. "An Inset CT Specimen for Evaluating Fracture in Small Samples of Material." *Science Direct*. N.p., n.d. Web. 12 Mar. 2014.

Appendices

Appendix 1. Force v Time graph. A typical fracture toughness force v time graph will display an initial increase in load much like a typical strength test, but will display a decrease in supported load as the crack propagates before failure (F). The peak value or point at which propagation begins is called the yield point (Y). This data is from one of the RTx bones in this study.

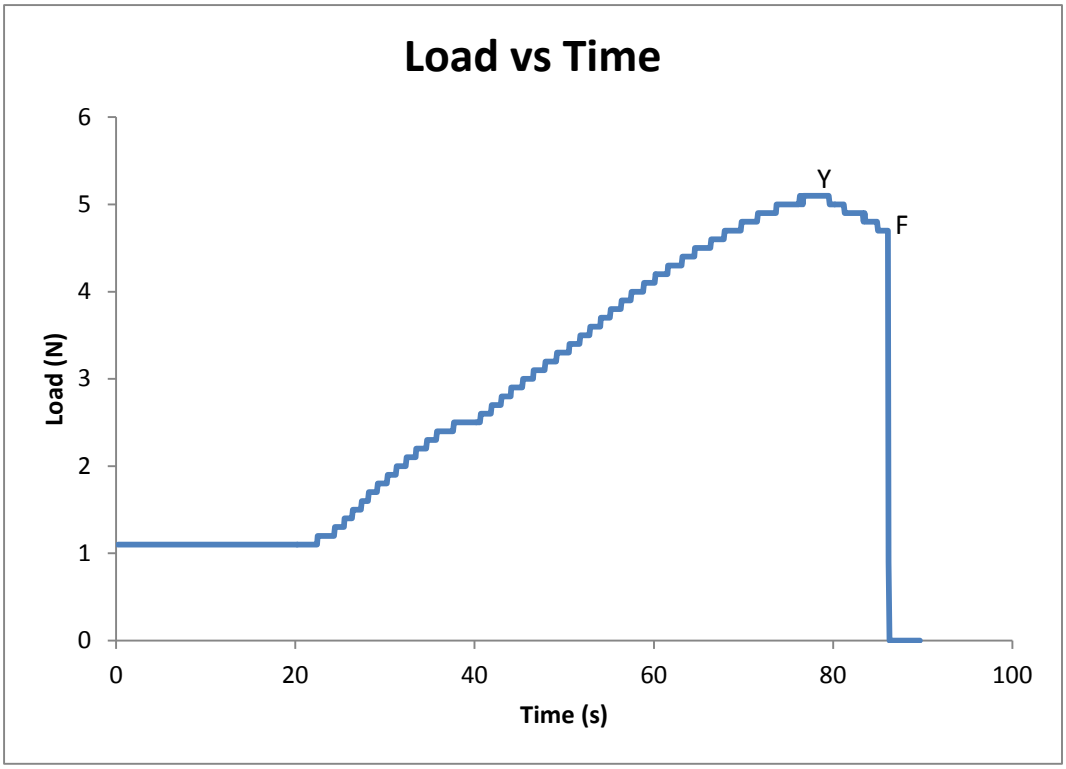

Appendix 2.

Initial crack length and critical fracture toughness correlation.